Agreement between the spatiotemporal gait parameters of healthy adults from the OptoGait© system and a traditional three-dimensional motion capture system.

Aoife Healy[1]
School of Life Sciences and Education, Staffordshire University
Science Centre, Staffordshire University, Stoke On Trent, ST4 2DF, UK.
a.healy@staffs.ac.uk

Kimberley Linyard-Tough
School of Life Sciences and Education, Staffordshire University
Science Centre, Staffordshire University, Stoke On Trent, ST4 2DF, UK.
kimberleymlt90@hotmail.co.uk

Nachiappan Chockalingam
School of Life Sciences and Education, Staffordshire University
Science Centre, Staffordshire University, Stoke On Trent, ST4 2DF, UK.
n.chockalingam@staffs.ac.uk

ABSTRACT

While previous research has assessed the validity of the OptoGait© system to the GAITRite© walkway and an instrumented treadmill, no research to date has assessed this system against a traditional three-dimensional motion analysis system. Additionally, previous research has shown that the OptoGait system shows systematic bias when compared to other systems due to the configuration of the system's hardware. The present study examined the agreement between the spatiotemporal gait parameters calculated from the OptoGait system and a three-dimensional motion capture (14 camera Vicon motion capture system and 2 AMTI force plates) in healthy adults. Additionally, a range of filter settings for the OptoGait were examined to determine if it was possible to eliminate any systematic bias between the OptoGait and the three-dimensional motion analysis system. Agreement between the systems was examined using 95% limits of agreement by Bland and Altman and the intraclass correlation coefficient. A repeated measures ANOVA were used to detect any systematic differences between the systems. Findings confirm the validity of the OptoGait system for the evaluation of spatiotemporal gait parameters in healthy adults. Furthermore, recommendations on filter settings which eliminate the systematic bias between the OptoGait and the three-dimensional motion analysis system are provided.

[1] Corresponding author

INTRODUCTION

The measurement of spatiotemporal gait parameters is commonly utilised to monitor change and assess the effect of treatment interventions in individuals [1,2]. Many of the systems used to measure spatiotemporal gait parameters are not easily portable and require a large area for measurement. The OptoGait system (Microgate, Italy) is a portable system which requires minimal time to set-up. It is a photoelectric system which detects the interruptions of the communication between the bars, caused by the participant's feet, to identify gait events (foot strike and foot off).

Previous research has assessed the validity of the OptoGait system, in relation to spatiotemporal gait parameters, against the GAITRite walkway [3,4] and an instrumented treadmill [5]. The reliability of the OptoGait system has also been confirmed [6], with the spatiotemporal gait parameters compared across two testing sessions which were two weeks apart. The authors confirmed that all parameters, except for acceleration and progressive step time assessment, were reliable.

The GAITRite walkway and instrumented treadmill have previously been validated against traditional three-dimensional motion analysis systems [7,8], however, to date the validity of the OptoGait system against three-dimensional motion analysis has not been assessed. Testing the OptoGait system's validity against three-dimensional motion analysis is warranted as the OptoGait utilises photoelectric sensors to calculate spatiotemporal gait parameters as opposed to the GAITRite and treadmill systems which are based on pressure sensing technology.

The OptoGait bars (with 96 LEDS per meter and a space resolution of 1.041 mm) are configured with the LEDs 3 mm from the ground, this results in the LEDs being interrupted a few milliseconds before contact with the ground. Similarly, when the foot is lifted from the ground during the foot off gait event, interruption with the LEDs is postponed. This has an effect on the calculation of the spatiotemporal gait parameters, with the calculated values from the OptoGait longer for the stance phase and shorter for the swing phase when compared to other gait analysis systems [3–5].

Filter settings (GaitR IN and OUT filter) within the OptoGait software allow the user to set the minimum number of LEDs to be interrupted for triggering the contact event. By changing this filter, it is proposed that it is possible to reduce or eliminate discrepancies between the OptoGait system and other gait analysis systems. The manufacturers of OptoGait recommend setting the filter to 3 LED, meaning that only when 4 consecutive LEDs are interrupted, the foot strike/foot off is considered valid. However, no research to date has examined the effect of different filter settings on the calculated spatiotemporal gait parameters. It is important to assess the effect of these different settings on the calculated gait parameters; to establish if specific settings would allow the results from different systems to be used interchangeably or if a correction factor would be required to eliminate the offset between the calculated gait parameters of different systems.

The main aim of this study was to examine the concurrent validity of the OptoGait system against a three-dimensional motion analysis system for the assessment of spatiotemporal gait parameters. Additionally, a range of filter settings for the

OptoGait were examined to determine the setting which most closely matched the measurements provided by the three-dimensional motion analysis system.

MATERIALS AND METHODS

PARTICIPANTS

Eighteen individuals (12 females and 6 males) volunteered to participate in the study (age: 31 ± 8 years; height: 170 ± 8 cm; weight 72 ± 17kg). Participants had no known medical conditions which would have affected their ability to participate in this study. The study was approved by the University ethics committee and consent was obtained from all individuals prior to participation.

PROCEDURE

A 5 m OptoGait system (sampling at 1000Hz; Microgate, Italy), two force plates (AMTI OPT464508HF sampling at 1000Hz; AMTI, USA) and a 14 camera Vicon motion capture system (sampling at 100Hz; Vicon, OMG, UK) were utilized for this study (Figure 1). To ensure participants has achieved steady state walking prior to data capture the OptoGait system was positioned in the centre of the laboratory with participants initiating gait 5-6 m before reaching the start of the OptoGait system. Participants walked across the laboratory at their self-selected speed (1.34 ± 0.18 ms-1) and completed as many trials as necessary to record five acceptable trials (i.e. five trials in which the participant's foot strikes contacted the two force plates). Participants were barefoot for this study and had reflective markers on their lateral malleoli and 2nd

metatarsal heads (dorsal side) to allow the calculation of gait events for the motion capture system.

IDENTIFICATION OF GAIT EVENTS AND CALCULATION OF GAIT PARAMETERS

Within the OptoGait system the default setting for the identification of gait events is when the first LED is interrupted (0 LED). The collected data was re-filtered in the OptoGait software (GaitR IN and OUT filter) with 1 LED (i.e. only when 1 additional LED interrupted is interrupted the gait event is considered valid), 2 LED and 3 LED settings (Figure 2).

For the motion capture system, the initial foot strike and foot off were identified by the force plates (threshold 20 N) and the two reflective markers on the feet, with the subsequent foot strike identified using the "Autocorrelate Events" pipeline within the Vicon Nexus software (Vicon Nexus version 2.4, Vicon, OMG, UK). This pipeline detects the pattern (vertical position) of the lateral malleolus marker at the gait events identified by the force plate and defines these events for the rest of the trial. The three-dimensional marker data were filtered with a Woltring filter (MSE=10) and no filter was applied to the force plate data."

The gait parameters for the motion capture system were calculated by Vicon Polygon software (Vicon Polygon version 4.3, Vicon, OMG, UK), with the distance parameters calculated from the position of the reflective marker placed on the 2nd metatarsal head (dorsal side). The OptoGait software (OptoGait version 1.8.10.0, Microgate, Italy) calculated the parameters for the OptoGait system.

ANALYSIS

Three trials for each participant were selected for analysis with the first right and left gait cycles (Figure 1) from each of the three trials included. A mean value for the eight spatiotemporal gait parameters (gait cycle, stance phase, swing phase, step time, step length, stride length, cadence, and walking speed) for these three trials, for both the left and right side, were calculated.

Agreement between the two systems was examined using 95% limits of agreement by Bland and Altman [9] and the intraclass correlation coefficient (ICC(2,1)). As a positive correlation was evident when the absolute differences between the systems were plotted against the individual means for the majority of the parameters, indicating heteroscedasticity in the data [10], the rate LOA (%LOA) [9] were calculated. A repeated measures ANOVA were used to detect any systematic differences between the systems, with statistical significance set at $p \leq 0.05$.

RESULTS

Results for the calculated spatiotemporal gait parameters from the three-dimensional motion capture system and the four OptoGait system settings (0 LED, 1 LED, 2 LED and 3 LED) are presented in Table 1. The ICC and %LOA comparing the motion capture system (Vicon+AMTI) to each of the four OptoGait system settings are also presented. Scatterplots and Bland–Altman plots for the eight spatiotemporal gait parameters provided by OptoGait against the three-dimensional motion capture system are presented in Supplementary File 1.

The repeated measures ANOVA with a Greenhouse-Geisser correction showed significant differences ($p \leq 0.05$) between the systems for stance phase, swing phase and walking speed, with results for the statistical analysis provided in Supplementary Table 1. . Post hoc tests using the Bonferroni correction revealed that differences were evident between the motion capture system (Vicon+AMTI) and OptoGait 0 LED and 1 LED filter settings for stance phase, swing phase and walking speed, with results for the statistical analysis provided in Supplementary Table 2. Stance phase timings were longer, swing phase was shorter and walking speed was slower for the OptoGait system settings compared to the motion capture system.

High concurrent validity was evident for most of the gait parameters between the four OptoGait system settings and the motion capture system with ICCs ranging from 0.690 and 0.999 ($p < 0.001$). Swing phase (left and right side) for Vicon+AMTI versus OptoGait 0 LED and left side swing phase for Vicon+AMTI versus OptoGait 3 LED were the only parameters with ICCs which were not considered excellent (i.e. less than 0.75). The %LOA were low for all gait parameters, for most the parameters the motion capture system measurement may differ from the OptoGait measurement by 2% below to 2% above. Slightly greater differences were evident for stance and swing phase parameters which may differ by 5% below to 5% above.

DISCUSSION

The four OptoGait system settings demonstrated high concurrent validity with the motion capture system based on the results of the ICCs and %LOA. However, a

significant systematic bias was evident between the motion capture system and the OptoGait 0 LED and 1 LED system settings for stance and swing phase and walking speed. These findings are in agreement with previous studies [3–5] and are attributed to the position of the LEDS on the OptoGait system, which are raised 3 mm from the ground. The value of the differences between the systems were small; the stance and swing phase gait parameters differed by a maximum 0.04s (OptoGait values were higher for stance phase and lower for swing phase), and walking speed was slower for OptoGait by a maximum of 0.007ms-1.

The systematic bias between the systems was eliminated when the 2 and 3 LED filter software settings were applied to the OptoGait system. While the ICCs for stance and swing phase were good to excellent for both these settings (2 and 3 LED), ICC values were higher for the 2 LED setting than the 3 LED setting. The range of the %LOA remained the same for stance phase across these two settings, with below 2% to above 5% for the 2 LED setting and below 5% to above 2% for the 3 LED setting. Differences in the %LOA were evident for swing phase results with below 2% to above 2% for the 2 LED setting and a higher range of below 2% to above 5% for the 3 LED setting. The ICCs and %LOA for walking speed were similar for the 2 and 3 LED settings.

At present, as the OptoGait is a relatively new system, there is a lack of normative variable values for the system. Results from the current study provide clinicians and researchers with confidence that the values provided by the OptoGait system can be compared to normative databases values, which are typically based on data from motion capture systems. In line with previous research, which confirmed the

validity of the spatiotemporal gait parameters from OptoGait system to other walkway and treadmill system [3–5], the current study demonstrates the high concurrent validity of the OptoGait system with a three-dimensional motion capture system.

While the present study has confirmed the validity of the OptoGait system for the evaluation of gait parameters in healthy adults additional research is required to confirm its validity for assessing pathologic populations. Previous research has confirmed its validity for assessing gait in individuals after total knee arthroplasty [3] and stroke [5].

CONCLUSIONS

Our findings confirm the validity of the OptoGait system for the evaluation of spatiotemporal gait parameters in healthy adults. Based on the study findings, when the OptoGait is utilized for research purposes, if gait parameters from the OptoGait system are to be compared to a three-dimensional motion capture system we recommend the use of the 2 LED filter setting, as the ICC values were higher for this setting than the 3 LED setting, within the OptoGait software.

ACKNOWLEDGMENT

The authors thank Microgate (Bolzano, Italy) for providing the OptoGait system for this study.

FUNDING

This research did not receive any specific grant from funding agencies in the public, commercial, or not-for-profit sectors.

CONFLICT OF INTEREST

Microgate (Bolzano, Italy) provided the OptoGait system for this study, however, they were not involved in the study design, data collection, analysis or interpretation of the data.

REFERENCES

[1] Jarvis, H. L., Bennett, A. N., Twiste, M., Phillip, R. D., Etherington, J., and Baker, R., 2017, "Temporal Spatial and Metabolic Measures of Walking in Highly Functional Individuals With Lower Limb Amputations," Arch. Phys. Med. Rehabil., **98**(7), pp. 1389–1399.

[2] Toosizadeh, N., Yen, T. C., Howe, C., Dohm, M., Mohler, J., and Najafi, B., 2015, "Gait Behaviors as an Objective Surgical Outcome in Low Back Disorders: A Systematic Review," Clin. Biomech., **30**(6), pp. 528–536.

[3] Lienhard, K., Schneider, D., and Maffiuletti, N. A., 2013, "Validity of the Optogait Photoelectric System for the Assessment of Spatiotemporal Gait Parameters," Med. Eng. Phys., **35**(4), pp. 500–504.

[4] Lee, M. M., Song, C. H., Lee, K. J., Jung, S. W., Shin, D. C., and Shin, S. H., 2014, "Concurrent Validity and Test-Retest Reliability of the OPTOGait Photoelectric Cell System for the Assessment of Spatio-Temporal Parameters of the Gait of Young Adults," J. Phys. Ther. Sci., **26**(1), pp. 81–85.

[5] Lee, M., Song, C., Lee, K., Shin, D., and Shin, S., 2014, "Agreement between the Spatio-Temporal Gait Parameters from Treadmill-Based Photoelectric Cell and the Instrumented Treadmill System in Healthy Young Adults and Stroke Patients.," Med. Sci. Monit., **20**, pp. 1210–9.

[6] Bernal., A. G., Becerro-de-Bengoa-Vallejo, R., and Losa-Iglesias, M. E., 2016, "Reliability of the OptoGait Portable Photoelectric Cell System for the Quantification of Spatial-Temporal Parameters of Gait in Young Adults," Gait Posture, **50**, pp. 196–200.

[7] Webster, K. E., Wittwer, J. E., and Feller, J. A., 2005, "Validity of the GAITRite Walkway System for the Measurement of Averaged and Individual Step Parameters of Gait.," Gait Posture, **22**(4), pp. 317–21.

[8] Reed, L. F., Urry, S. R., and Wearing, S. C., 2013, "Reliability of Spatiotemporal and Kinetic Gait Parameters Determined by a New Instrumented Treadmill System," BMC Musculoskelet. Disord., **14**(1), p. 249.

[9] Bland, M. J., and Altman, D. J., 1986, "Statistical Methods for Assessing Agreement between Two Methods of Clinical Measurement," Lancet, **1**(fig 1), pp. 307–310.

[10] Atkinson, G., and Nevill, A., 1998, "Statistical Methods for Assssing Measurement Error (Reliability) in Variables Relevant to Sports Medicine," Sport. Med., **26**(4), pp. 217–238.

Figure Captions List

Fig. 1 Testing setup with two force plates at the start of the 5m OptoGait system

Fig. 2 OptoGait LED filter settings (a) 0 LED, (b) 1 LED, (c) 2 LED and (d) 3 LED. These settings indicate the number of additional LED sensors they must be interrupted by the foot to trigger the start/end of the foot contact time.

Table Caption List

Table 1 Concurrent validity of the four OptoGait system settings (0 LED, 1 LED, 2 LED and 3 LED) with the 3D motion capture system (Vicon+AMTI) for gait parameters.

Figure 1

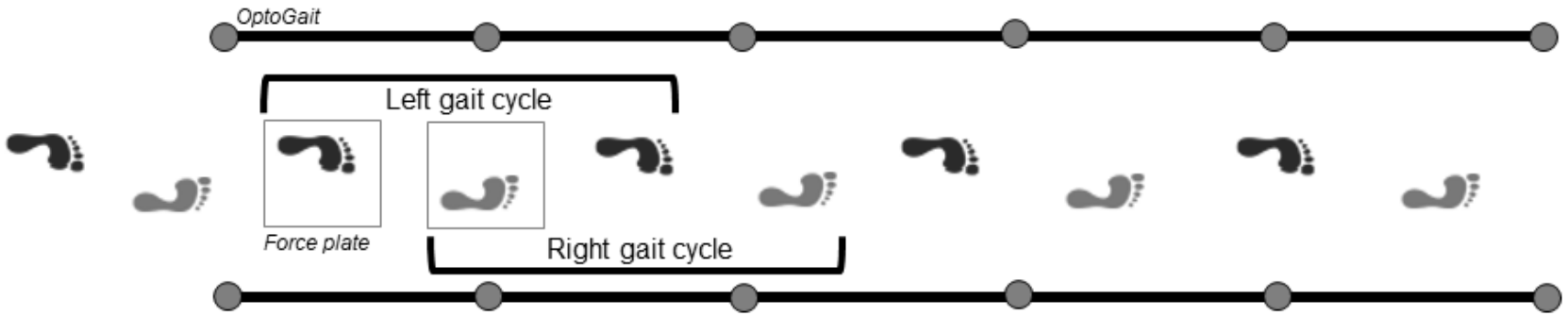

Figure 2

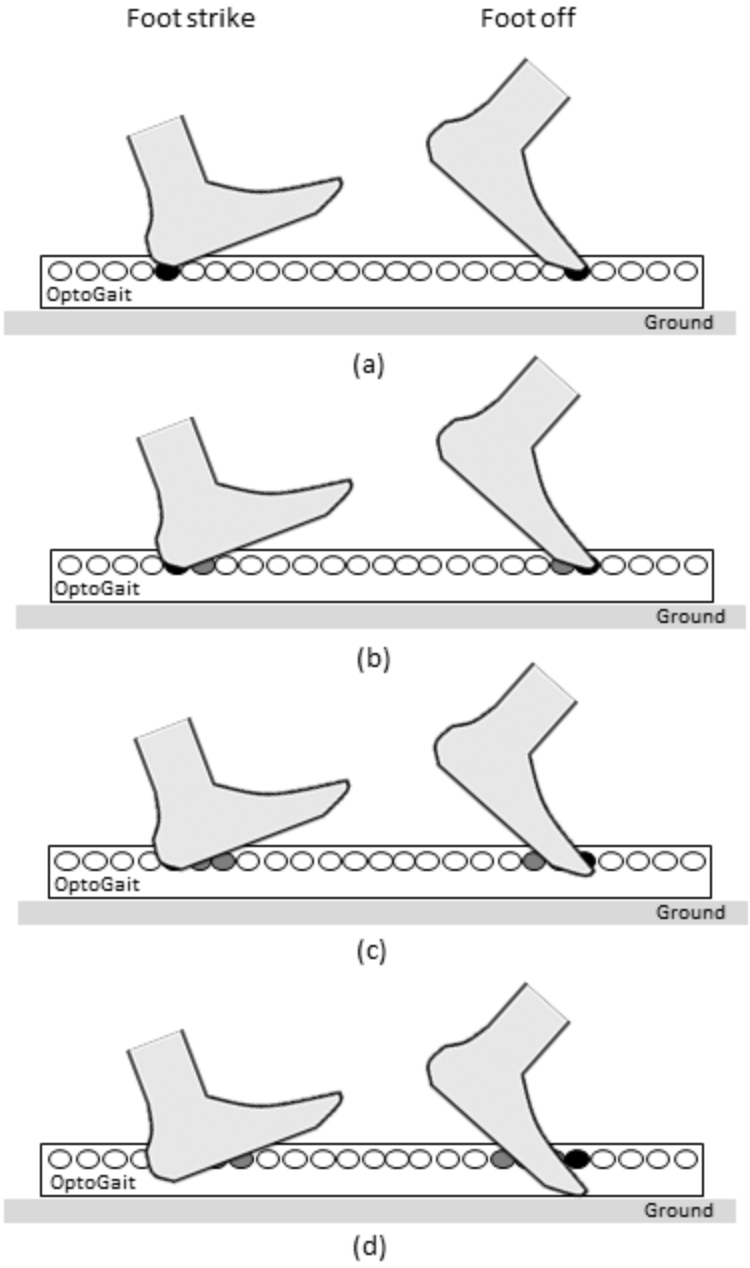
Foot strike
Foot off
OptoGait
Ground
(a)
OptoGait
Ground
(b)
OptoGait
Ground
(c)
OptoGait
Ground
(d)

Table 1

LEFT SIDE	Vicon+AMTI	OptoGait (0 LED)			OptoGait (1 LED)			OptoGait (2 LED)			OptoGait (3 LED)		
	mean ± SD	mean ± SD	ICC (95% confidence intervals)	%LOA	mean ± SD	ICC (95% confidence intervals)	%LOA	mean ± SD	ICC (95% confidence intervals)	%LOA	mean ± SD	ICC (95% confidence intervals)	%LOA
Gait cycle (s)	1.04 ± 0.08	1.05 ± 0.07	0.989 (0.97 - 0.996)	-2% - 2%	1.05 ± 0.08	0.989 (0.97 - 0.996)	-2% - 2%	1.04 ± 0.08	0.991 (0.977 - 0.997)	-2% - 2%	1.05 ± 0.08	0.991 (0.975 - 0.996)	-2% - 2%
Stance phase (s)	0.63 ± 0.05	0.66 ± 0.05*	0.936 (-0.043 - 0.988)	0% - 5%	0.65 ± 0.06*	0.961 (0.09 - 0.992)	-2% - 5%	0.63 ± 0.06	0.983 (0.955 - 0.994)	-2% - 5%	0.62 ± 0.07	0.955 (0.865 - 0.984)	-5% - 2%
Swing phase (s)	0.41 ± 0.02	0.39 ± 0.02*	0.735 (-0.197 - 0.933)	-5% - 2%	0.40 ± 0.02*	0.821 (0.054 - 0.949)	-5% - 2%	0.41 ± 0.02	0.831 (0.543 - 0.937)	-2% - 2%	0.43 ± 0.03	0.717 (0.218 - 0.895)	-2% - 5%
Step time (s)	0.52 ± 0.04	0.52 ± 0.04	0.980 (0.946 - 0.992)	-2% - 2%	0.52 ± 0.04	0.980 (0.946 - 0.992)	-2% - 2%	0.52 ± 0.04	0.980 (0.946 - 0.992)	-2% - 2%	0.52 ± 0.04	0.978 (0.942 - 0.992)	-2% - 2%
Step length (m)	0.69 ± 0.05	0.69 ± 0.05	0.985 (0.955 - 0.995)	-2% - 2%	0.69 ± 0.05	0.985 (0.96 - 0.994)	-2% - 2%	0.69 ± 0.05	0.988 (0.965 - 0.995)	-2% - 2%	0.69 ± 0.05	0.987 (0.962 - 0.995)	-2% - 2%
Stride length (m)	1.39 ± 0.10	1.38 ± 0.10	0.999 (0.997 - 1)	-2% - 2%	1.38 ± 0.10	0.999 (0.997 - 1)	-2% - 2%	1.38 ± 0.10	0.998 (0.996 - 0.999)	-2% - 2%	1.38 ± 0.10	0.998 (0.995 - 0.999)	-2% - 2%
Cadence (steps per minute)	116 ± 9	115 ± 8	0.996 (0.987 - 0.998)	-2% - 2%	115 ± 8	0.996 (0.99 - 0.999)	-2% - 2%	115 ± 8	0.996 (0.99 - 0.999)	-2% - 2%	116 ± 9	0.996 (0.991 - 0.999)	-2% - 2%
Walking Speed (ms^{-1})	1.339 ± 0.180	1.333 ± 0.180*	0.999 (0.995 - 1)	-2% - 2%	1.334 ± 0.180*	0.999 (0.996 - 1)	-2% - 2%	1.336 ± 0.178	0.999 (0.999 - 1)	0% - 0%	1.338 ± 0.182	1 (0.999 - 1)	-2% - 0%
RIGHT SIDE													
Gait cycle (s)	1.04 ± 0.08	1.04 ± 0.08	0.994 (0.975 - 0.998)	-2% - 2%	1.04 ± 0.08	0.994 (0.981 - 0.998)	-2% - 2%	1.04 ± 0.08	0.994 (0.979 - 0.998)	-2% - 2%	1.04 ± 0.08	0.995 (0.986 - 0.998)	-2% - 2%
Stance phase (s)	0.62 ± 0.06	0.66 ± 0.06*	0.909 (-0.097 - 0.981)	-2% - 5%	0.65 ± 0.06*	0.944 (0.311 - 0.986)	-2% - 5%	0.63 ± 0.06	0.967 (0.911 - 0.988)	-2% - 5%	0.62 ± 0.06	0.967 (0.916 - 0.988)	-5% - 2%
Swing phase (s)	0.41 ± 0.03	0.39 ± 0.02*	0.690 (-0.224 - 0.915)	-5% - 0%	0.40 ± 0.03*	0.758 (0.074 - 0.922)	-5% - 2%	0.41 ± 0.03	0.863 (0.637 - 0.949)	-2% - 2%	0.42 ± 0.03	0.769 (0.396 - 0.913)	-2% - 5%
Step time (s)	0.52 ± 0.04	0.52 ± 0.04	0.975 (0.925 - 0.991)	-2% - 2%	0.52 ± 0.04	0.971 (0.924 - 0.989)	-2% - 2%	0.52 ± 0.04	0.975 (0.929 - 0.991)	-2% - 2%	0.52 ± 0.04	0.978 (0.936 - 0.992)	-2% - 2%
Step length (m)	0.69 ± 0.06	0.70 ± 0.05	0.992 (0.98 - 0.997)	-2% - 2%	0.7 ± 0.05	0.992 (0.979 - 0.997)	-2% - 2%	0.70 ± 0.05	0.992 (0.979 - 0.997)	-2% - 2%	0.70 ± 0.05	0.992 (0.986 - 0.997)	-2% - 2%
Stride length (m)	1.39 ± 0.11	1.39 ± 0.10	0.999 (0.996 - 0.999)	-2% - 2%	1.39 ± 0.10	0.998 (0.995 - 0.999)	-2% - 2%	1.39 ± 0.10	0.999 (0.996 - 0.999)	-2% - 2%	1.39 ± 0.10	0.998 (0.996 - 0.999)	-2% - 2%
Cadence (steps per minute)	116 ± 9	116 ± 9	0.996 (0.981 - 0.999)	-2% - 2%	116 ± 9	0.995 (0.983 - 0.998)	-2% - 2%	116 ± 9	0.996 (0.984 - 0.999)	-2% - 2%	116 ± 9	0.996 (0.986 - 0.998)	-2% - 2%
Walking Speed (ms^{-1})	1.353 ± 0.182	1.346 ± 0.178*	0.999 (0.992 - 1)	-2% - 2%	1.346 ± 0.178*	0.999 (0.991 - 1)	-2% - 2%	1.346 ± 0.177	0.999 (0.994 - 1)	-2% - 2%	1.347 ± 0.179	0.999 (0.996 - 1)	-2% - 2%

*Significant difference between OptoGait and Vicon+AMTI.
ICC = Intraclass correlation coefficient; LOA = Limits of agreement

Supplementary material

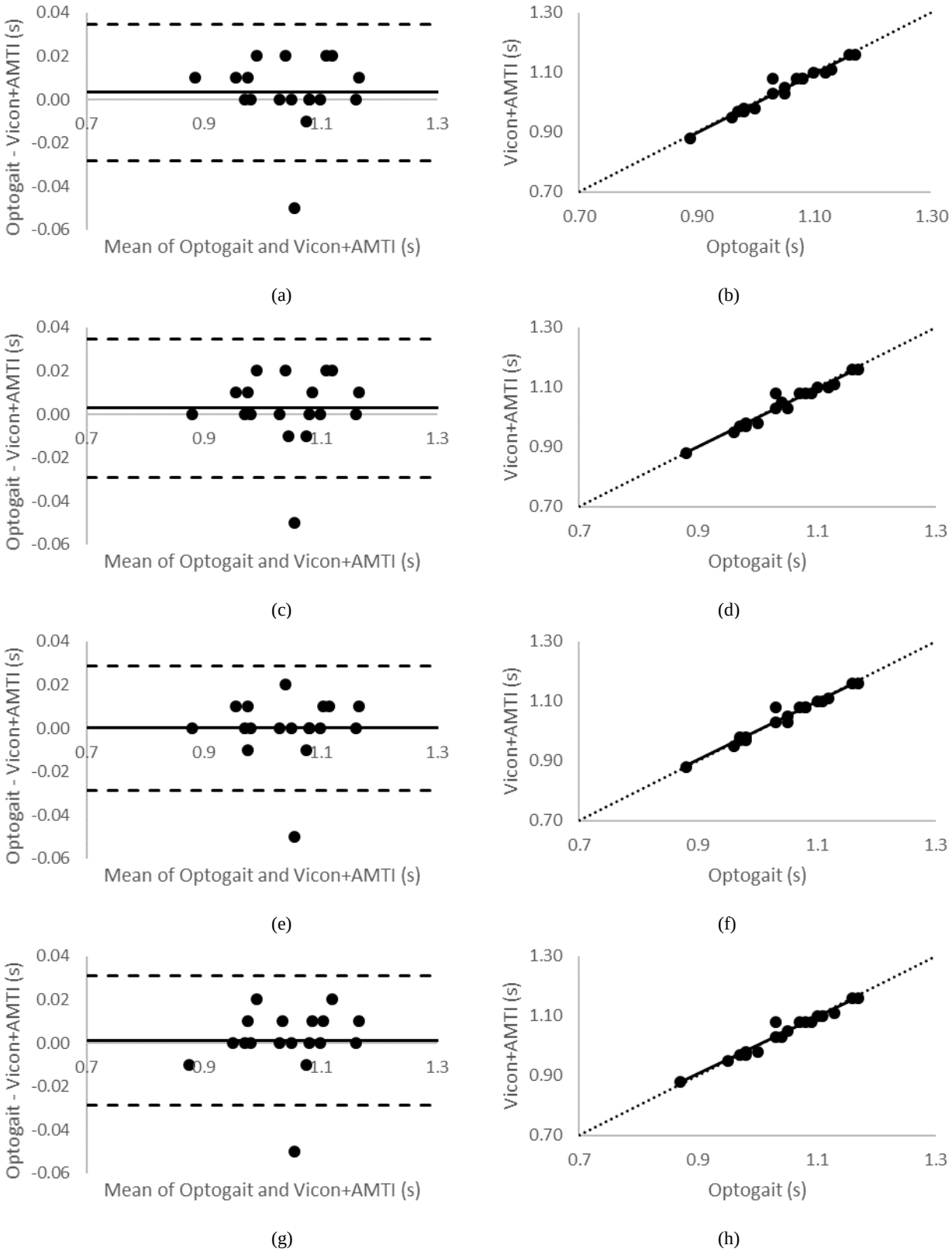

Supplementary Figure 1: Bland–Altman plots and scatterplots for left side gait cycle (s) Vicon+AMTI against 0 LED (a and b), 1 LED (c and d), 2 LED (e and f) and 3 LED (g and h). On the Bland–Altman plots, the solid line represents the bias and the broken lines represent the upper and lower 95% Limits of Agreement. On the scatterplots, the solid line represents the linear regression line and the dotted line represents the identity line.

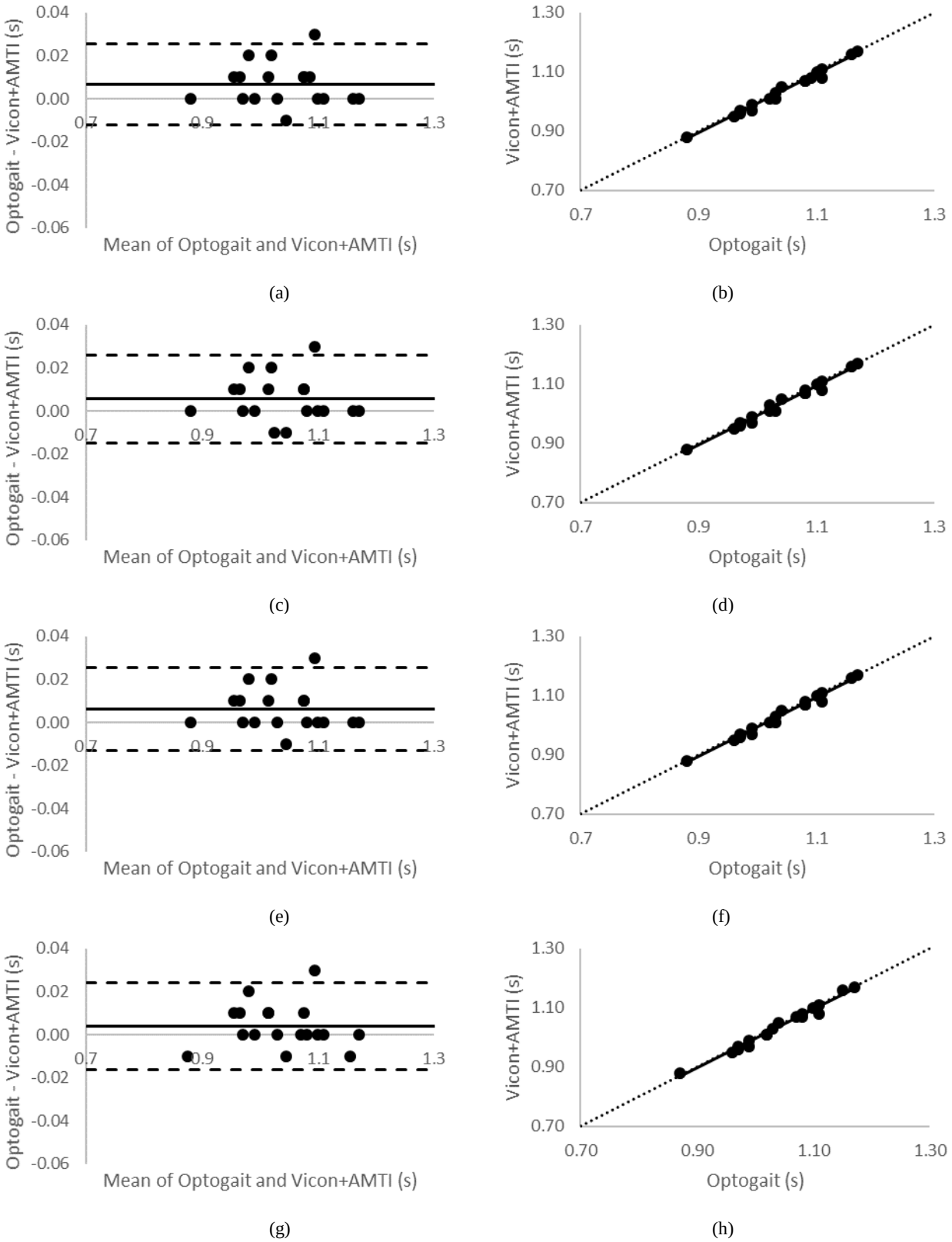

Supplementary Figure 2: Bland–Altman plots and scatterplots for right side gait cycle (s) Vicon+AMTI against 0 LED (a and b), 1 LED (c and d), 2 LED (e and f) and 3 LED (g and h). On the Bland–Altman plots, the solid line represents the bias and the broken lines represent the upper and lower 95% Limits of Agreement. On the scatterplots, the solid line represents the linear regression line and the dotted line represents the identity line.

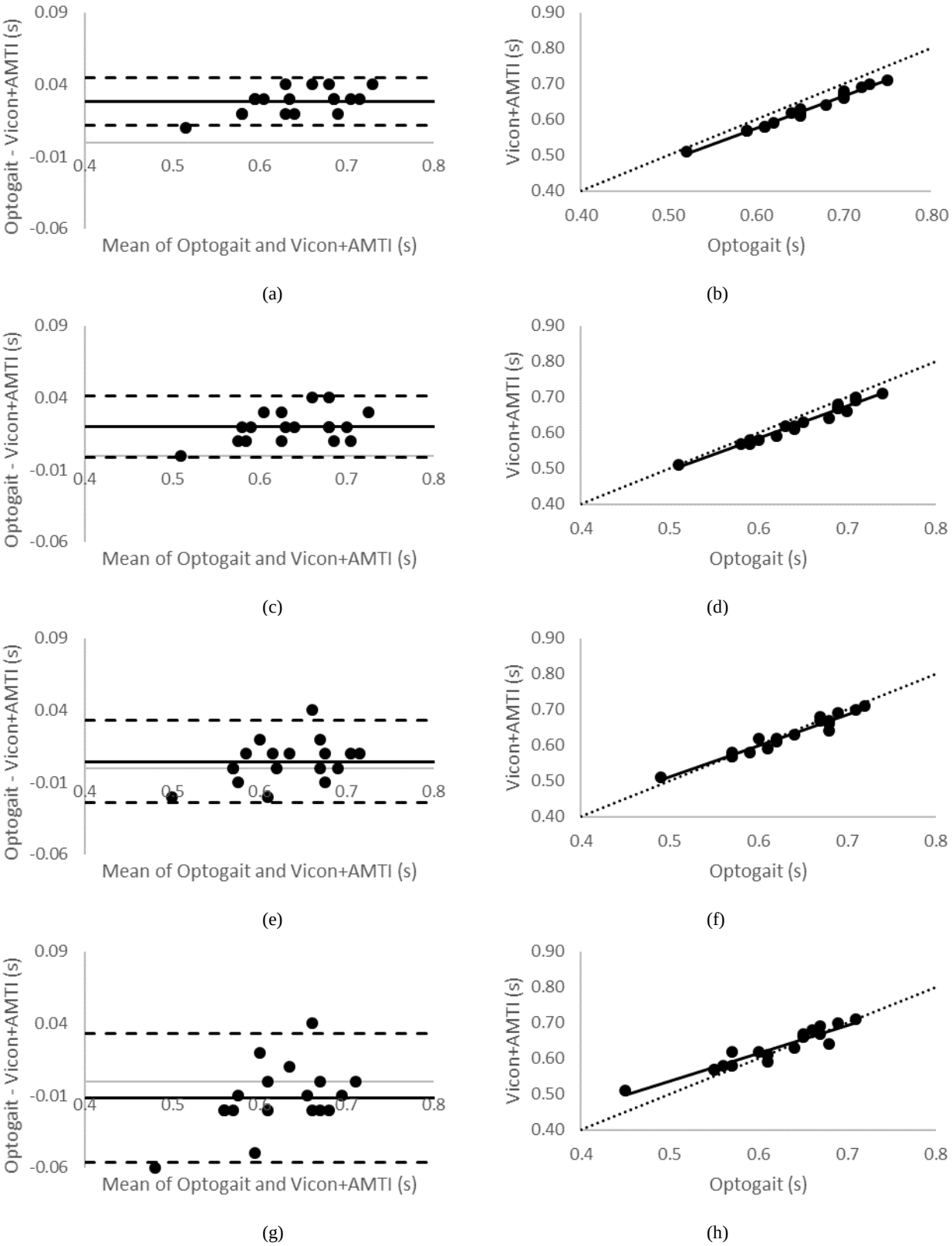

Supplementary Figure 3: Bland–Altman plots and scatterplots for left stance phase (s) Vicon+AMTI against 0 LED (a and b), 1 LED (c and d), 2 LED (e and f) and 3 LED (g and h). On the Bland–Altman plots, the solid line represents the bias and the broken lines represent the upper and lower 95% Limits of Agreement. On the scatterplots, the solid line represents the linear regression line and the dotted line represents the identity line.

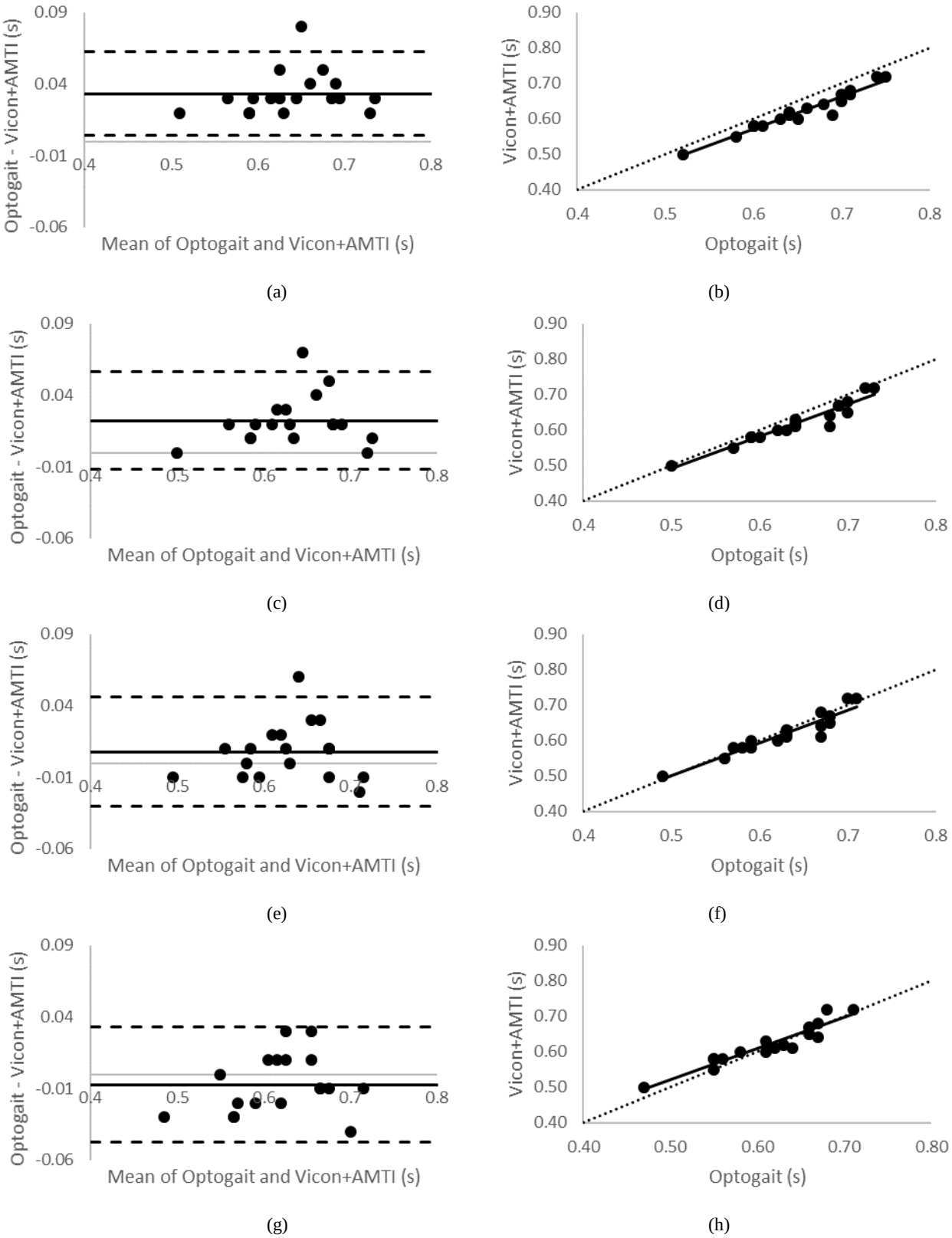

Supplementary Figure 4: Bland–Altman plots and scatterplots for right stance phase (s) Vicon+AMTI against 0 LED (a and b), 1 LED (c and d), 2 LED (e and f) and 3 LED (g and h). On the Bland–Altman plots, the solid line represents the bias and the broken lines represent the upper and lower 95% Limits of Agreement. On the scatterplots, the solid line represents the linear regression line and the dotted line represents the identity line.

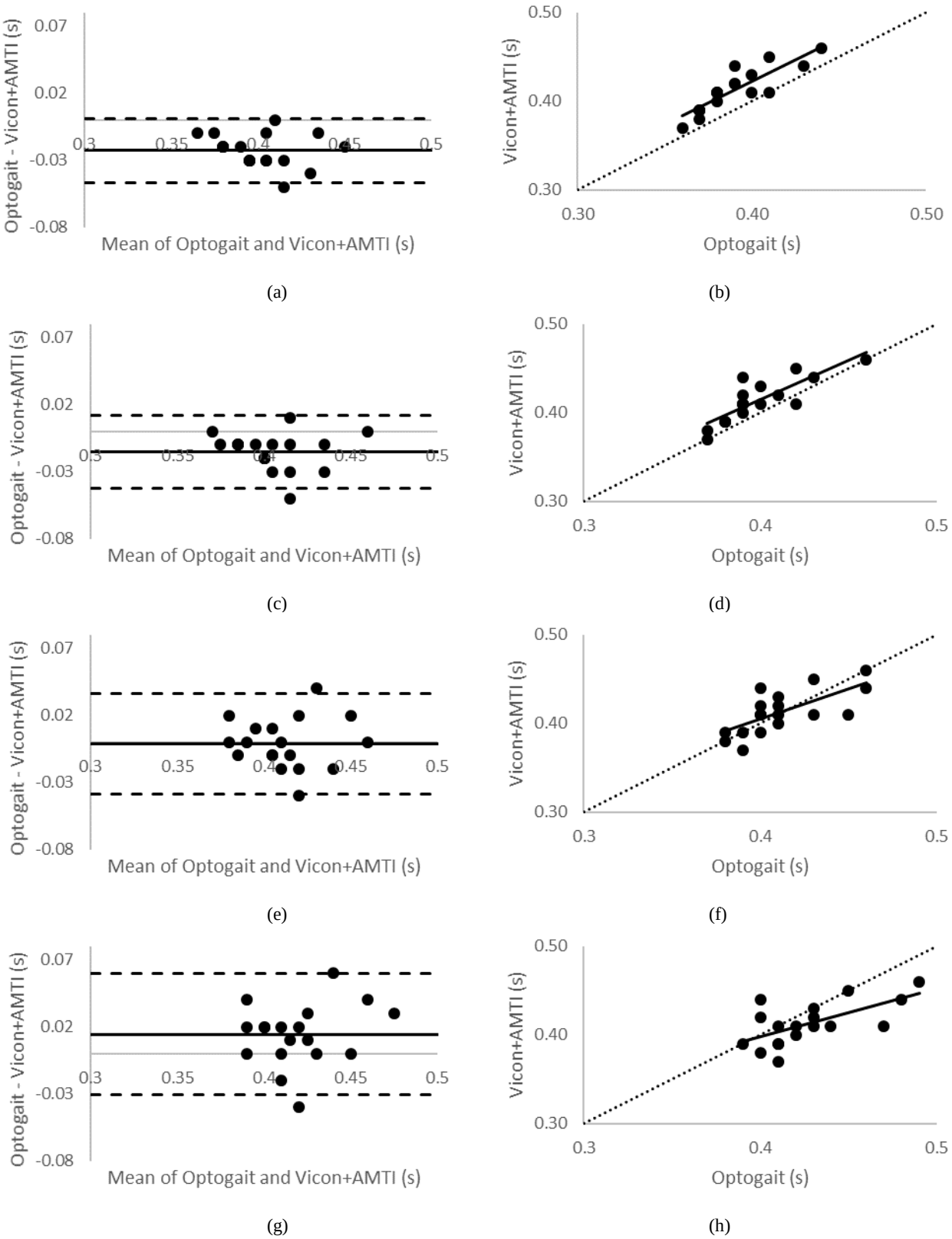

Supplementary Figure 5: Bland–Altman plots and scatterplots for left swing phase (s) Vicon+AMTI against 0 LED (a and b), 1 LED (c and d), 2 LED (e and f) and 3 LED (g and h). On the Bland–Altman plots, the solid line represents the bias and the broken lines represent the upper and lower 95% Limits of Agreement. On the scatterplots, the solid line represents the linear regression line and the dotted line represents the identity line.

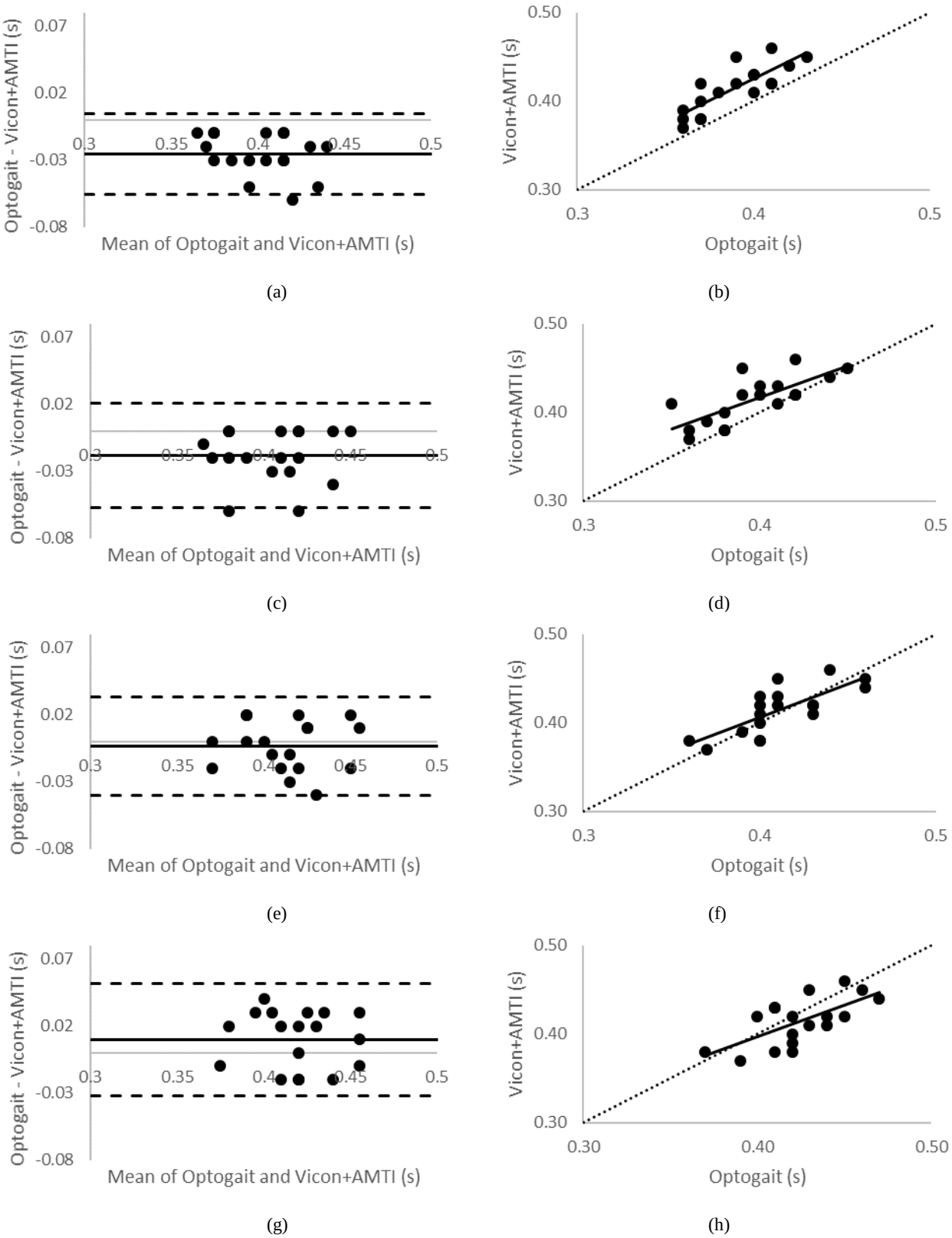

Supplementary Figure 6: Bland–Altman plots and scatterplots for right swing phase (s) Vicon+AMTI against 0 LED (a and b), 1 LED (c and d), 2 LED (e and f) and 3 LED (g and h). On the Bland–Altman plots, the solid line represents the bias and the broken lines represent the upper and lower 95% Limits of Agreement. On the scatterplots, the solid line represents the linear regression line and the dotted line represents the identity line.

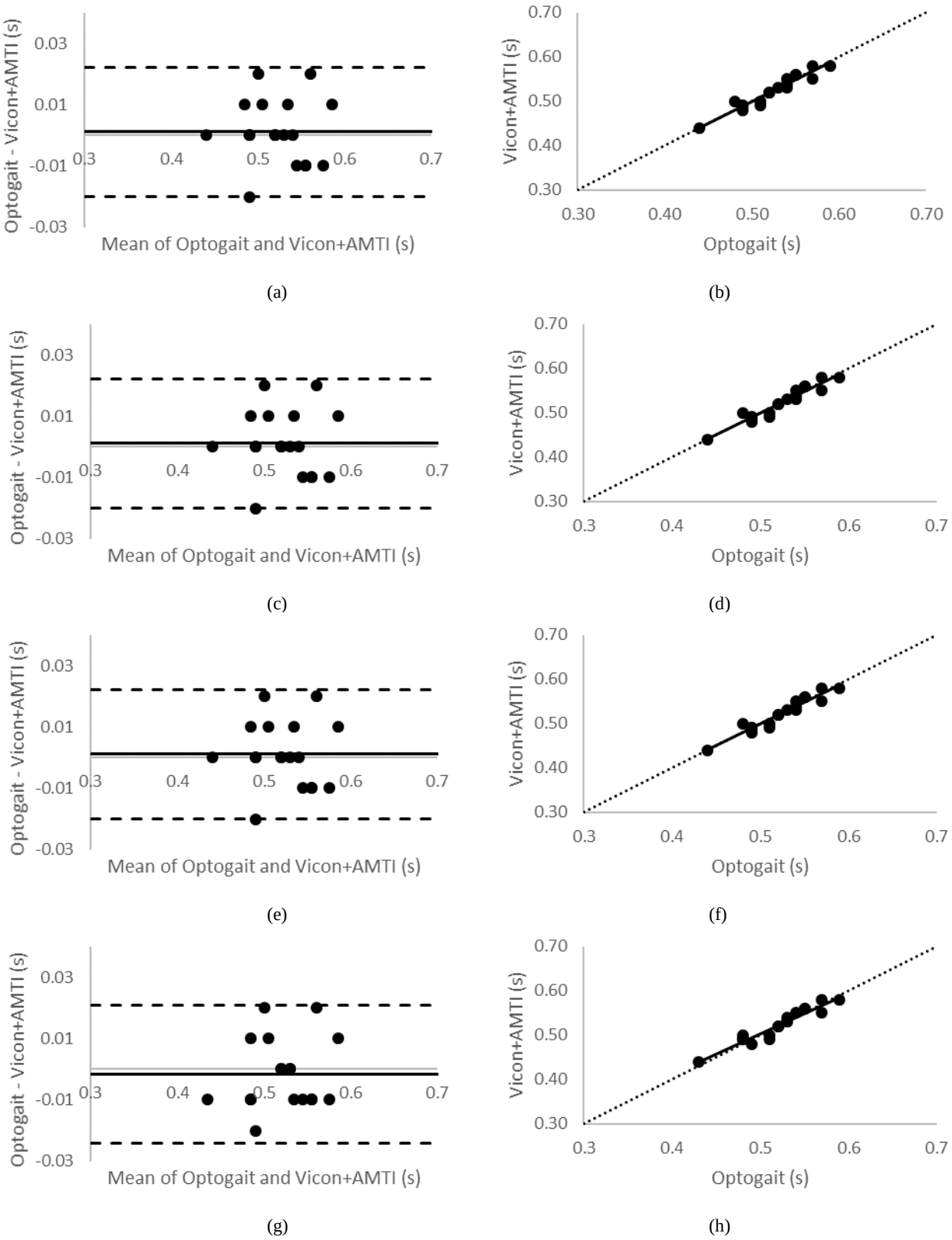

Supplementary Figure 7: Bland–Altman plots and scatterplots for left step time (s) Vicon+AMTI against 0 LED (a and b), 1 LED (c and d), 2 LED (e and f) and 3 LED (g and h). On the Bland–Altman plots, the solid line represents the bias and the broken lines represent the upper and lower 95% Limits of Agreement. On the scatterplots, the solid line represents the linear regression line and the dotted line represents the identity line.

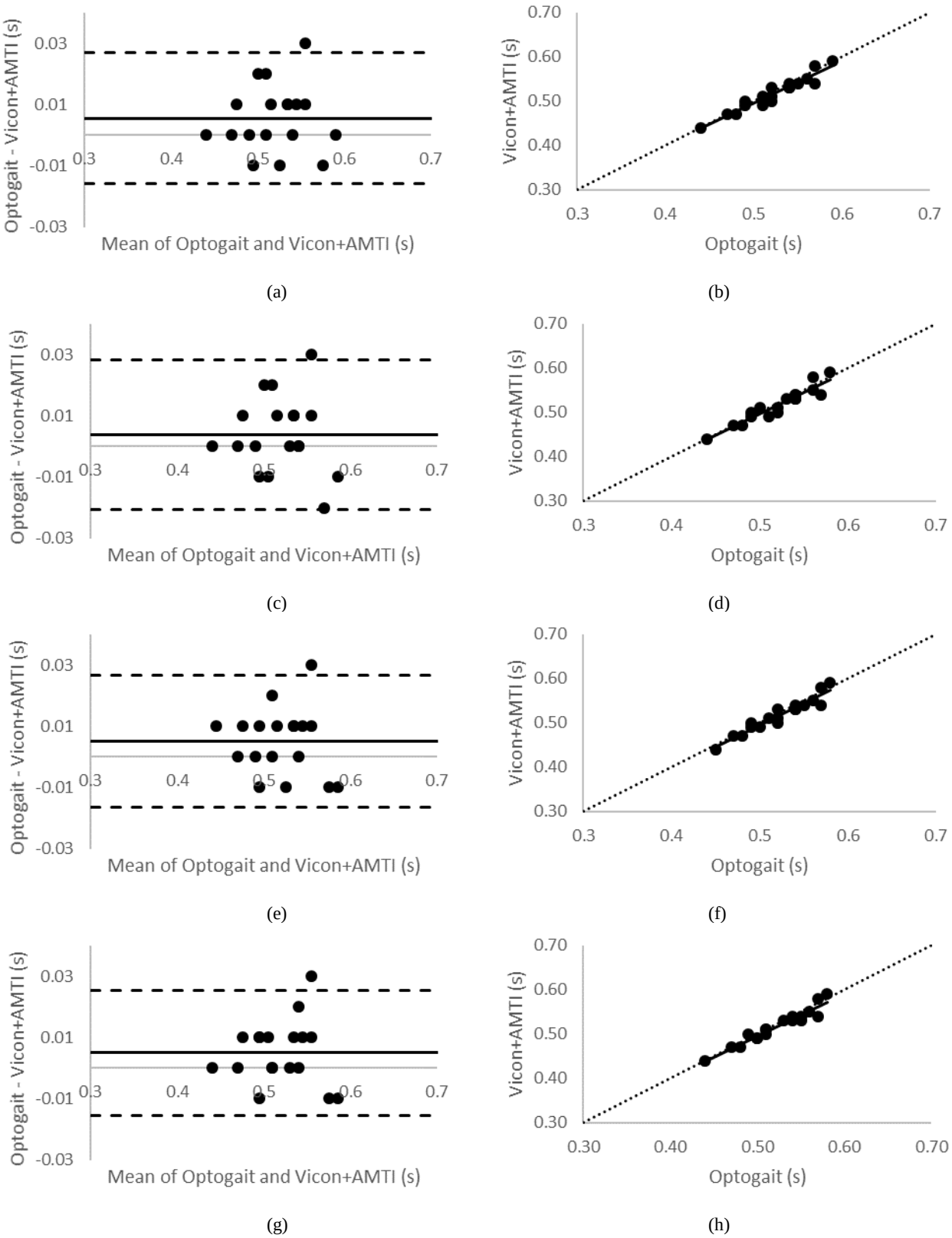

Supplementary Figure 8: Bland–Altman plots and scatterplots for right step time (s) Vicon+AMTI against 0 LED (a and b), 1 LED (c and d), 2 LED (e and f) and 3 LED (g and h). On the Bland–Altman plots, the solid line represents the bias and the broken lines represent the upper and lower 95% Limits of Agreement. On the scatterplots, the solid line represents the linear regression line and the dotted line represents the identity line.

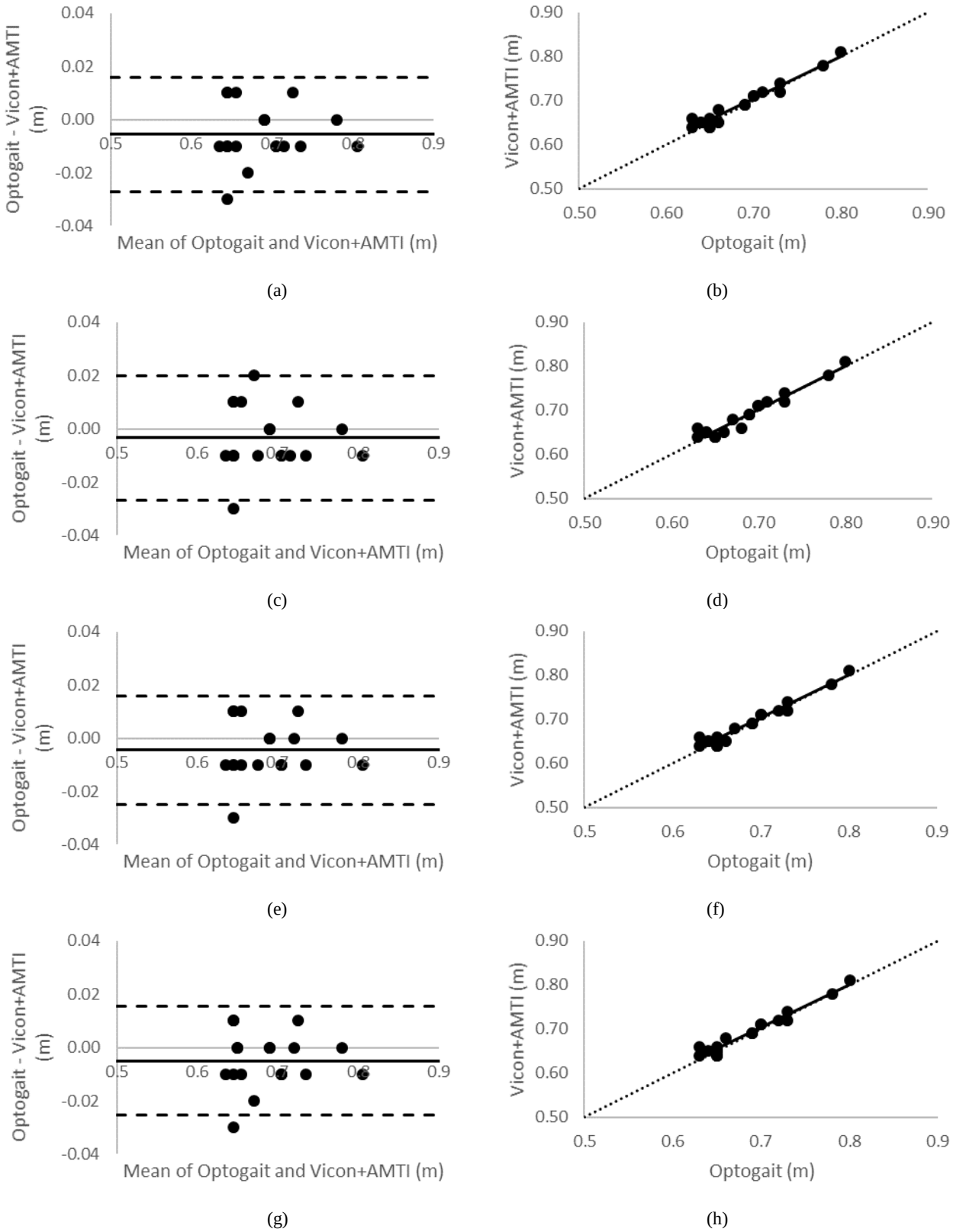

Supplementary Figure 9: Bland–Altman plots and scatterplots for left step length (m) Vicon+AMTI against 0 LED (a and b), 1 LED (c and d), 2 LED (e and f) and 3 LED (g and h). On the Bland–Altman plots, the solid line represents the bias and the broken lines represent the upper and lower 95% Limits of Agreement. On the scatterplots, the solid line represents the linear regression line and the dotted line represents the identity line.

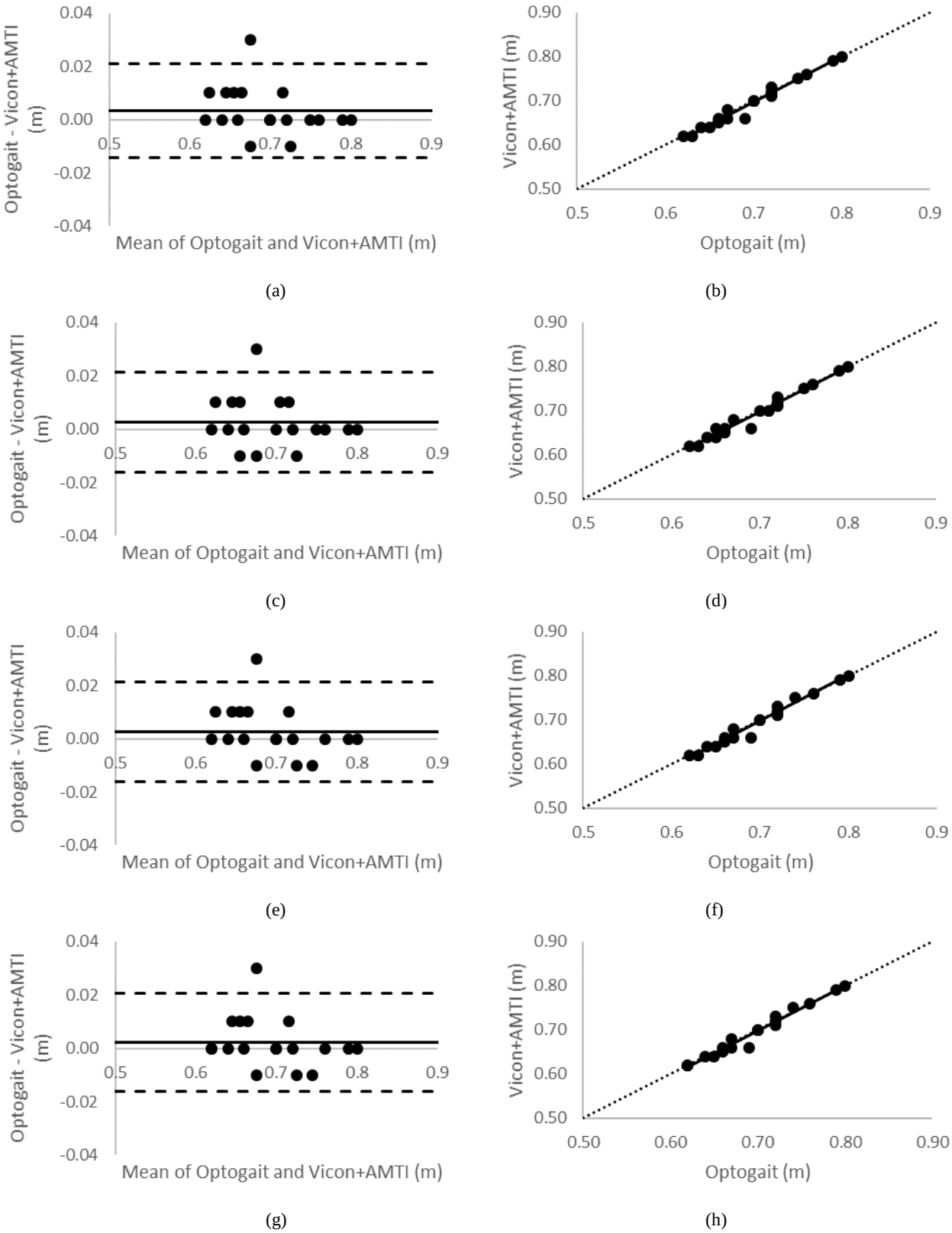

Supplementary Figure 10: Bland–Altman plots and scatterplots for right step length (m) Vicon+AMTI against 0 LED (a and b), 1 LED (c and d), 2 LED (e and f) and 3 LED (g and h). On the Bland–Altman plots, the solid line represents the bias and the broken lines represent the upper and lower 95% Limits of Agreement. On the scatterplots, the solid line represents the linear regression line and the dotted line represents the identity line.

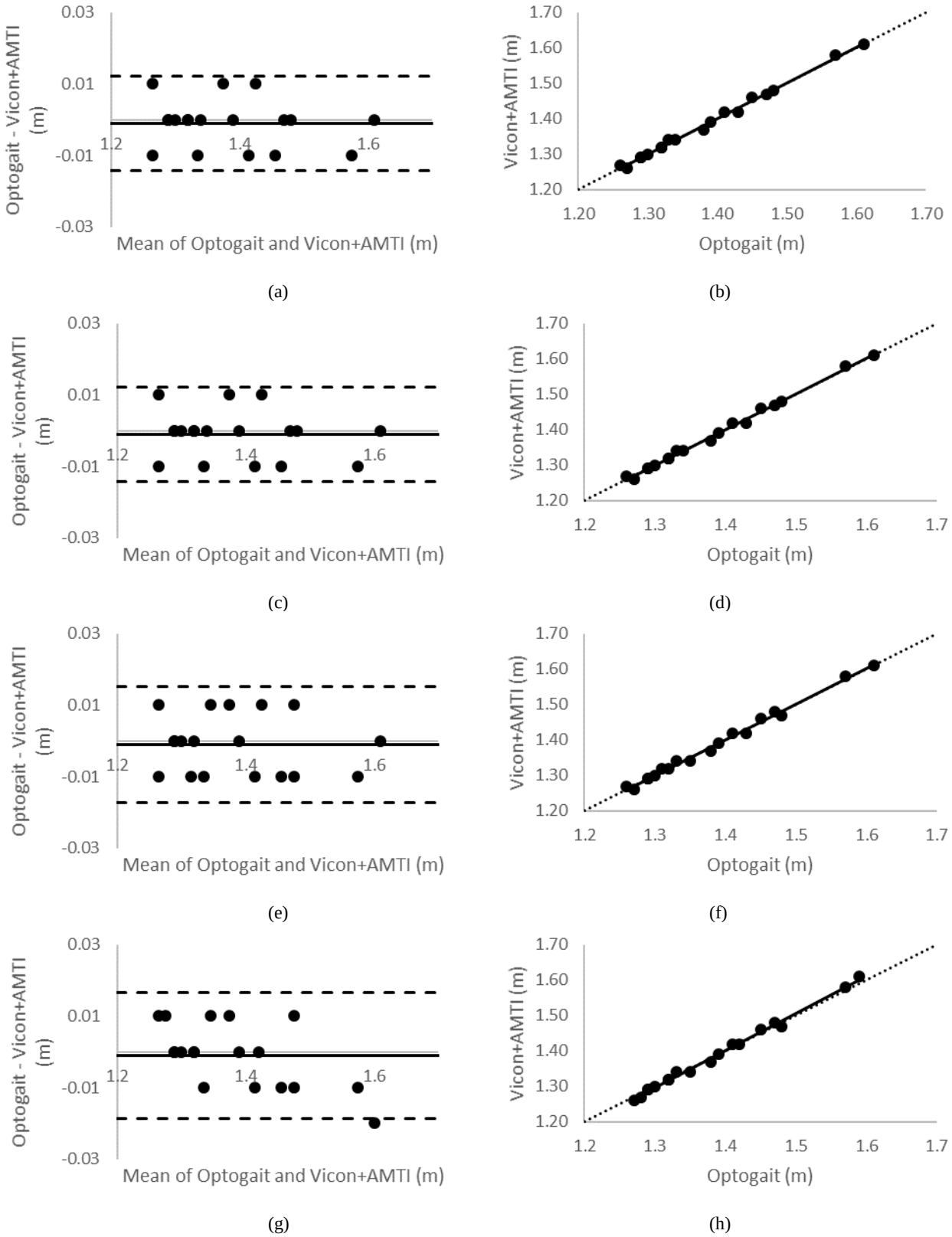

Supplementary Figure 11: Bland–Altman plots and scatterplots for left stride length (m) Vicon+AMTI against 0 LED (a and b), 1 LED (c and d), 2 LED (e and f) and 3 LED (g and h). On the Bland–Altman plots, the solid line represents the bias and the broken lines represent the upper and lower 95% Limits of Agreement. On the scatterplots, the solid line represents the linear regression line and the dotted line represents the identity line.

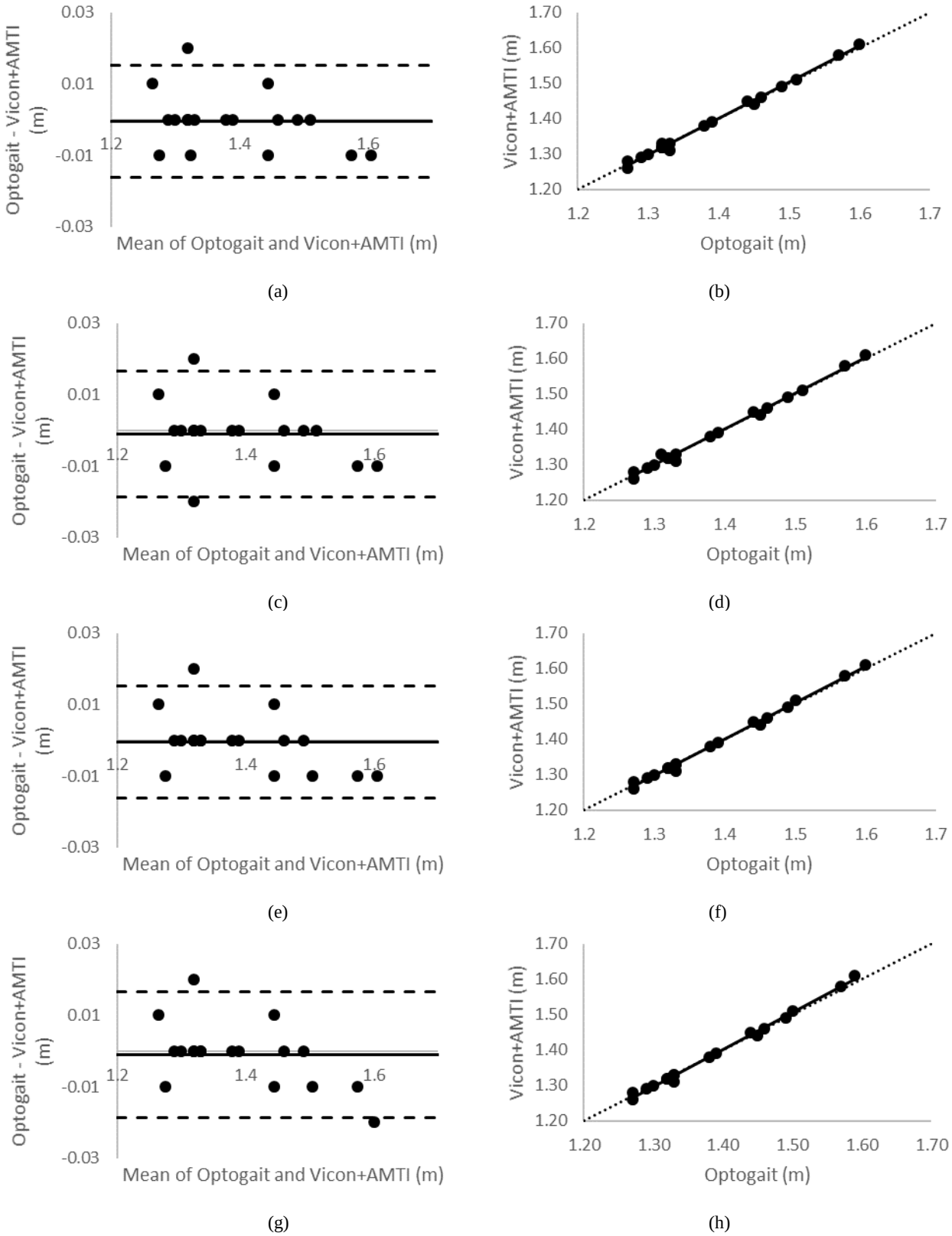

Supplementary Figure 12: Bland–Altman plots and scatterplots for right stride length (m) Vicon+AMTI against 0 LED (a and b), 1 LED (c and d), 2 LED (e and f) and 3 LED (g and h). On the Bland–Altman plots, the solid line represents the bias and the broken lines represent the upper and lower 95% Limits of Agreement. On the scatterplots, the solid line represents the linear regression line and the dotted line represents the identity line.

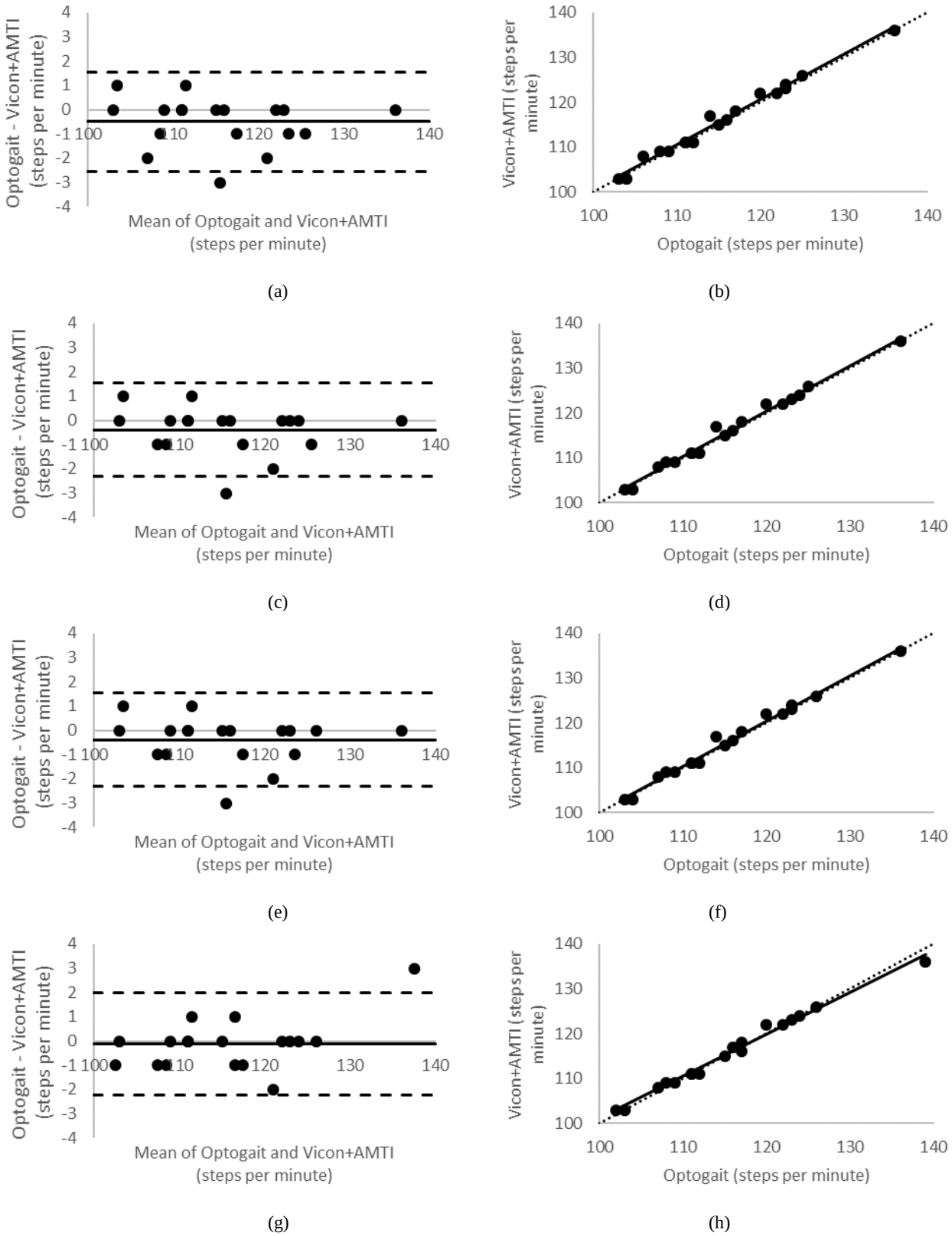

Supplementary Figure 13: Bland–Altman plots and scatterplots for left cadence (steps per minute) Vicon+AMTI against 0 LED (a and b), 1 LED (c and d), 2 LED (e and f) and 3 LED (g and h). On the Bland–Altman plots, the solid line represents the bias and the broken lines represent the upper and lower 95% Limits of Agreement. On the scatterplots, the solid line represents the linear regression line and the dotted line represents the identity line.

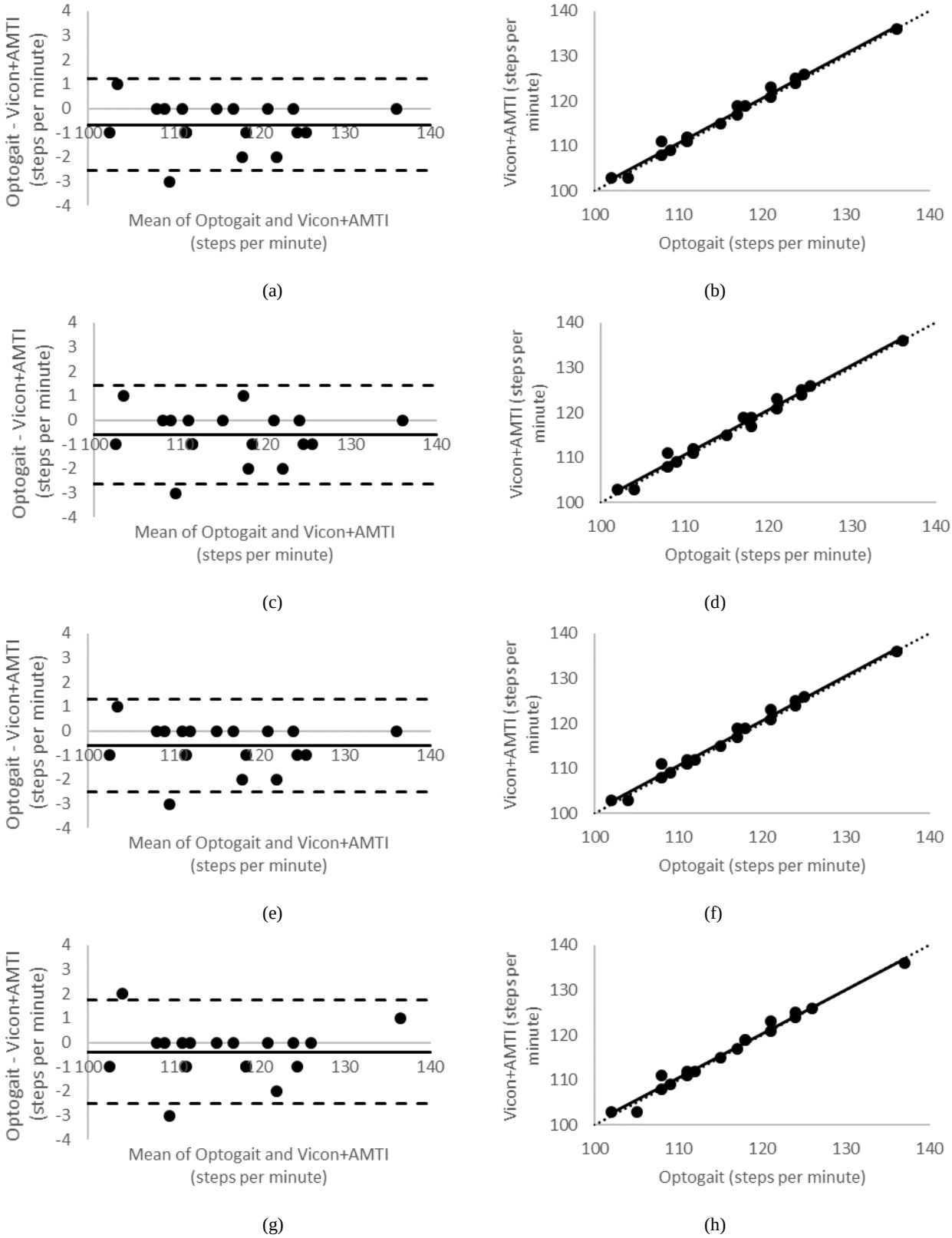

Supplementary Figure 14: Bland–Altman plots and scatterplots for right cadence (steps per minute) Vicon+AMTI against 0 LED (a and b), 1 LED (c and d), 2 LED (e and f) and 3 LED (g and h). On the Bland–Altman plots, the solid line represents the bias and the broken lines represent the upper and lower 95% Limits of Agreement. On the scatterplots, the solid line represents the linear regression line and the dotted line represents the identity line.

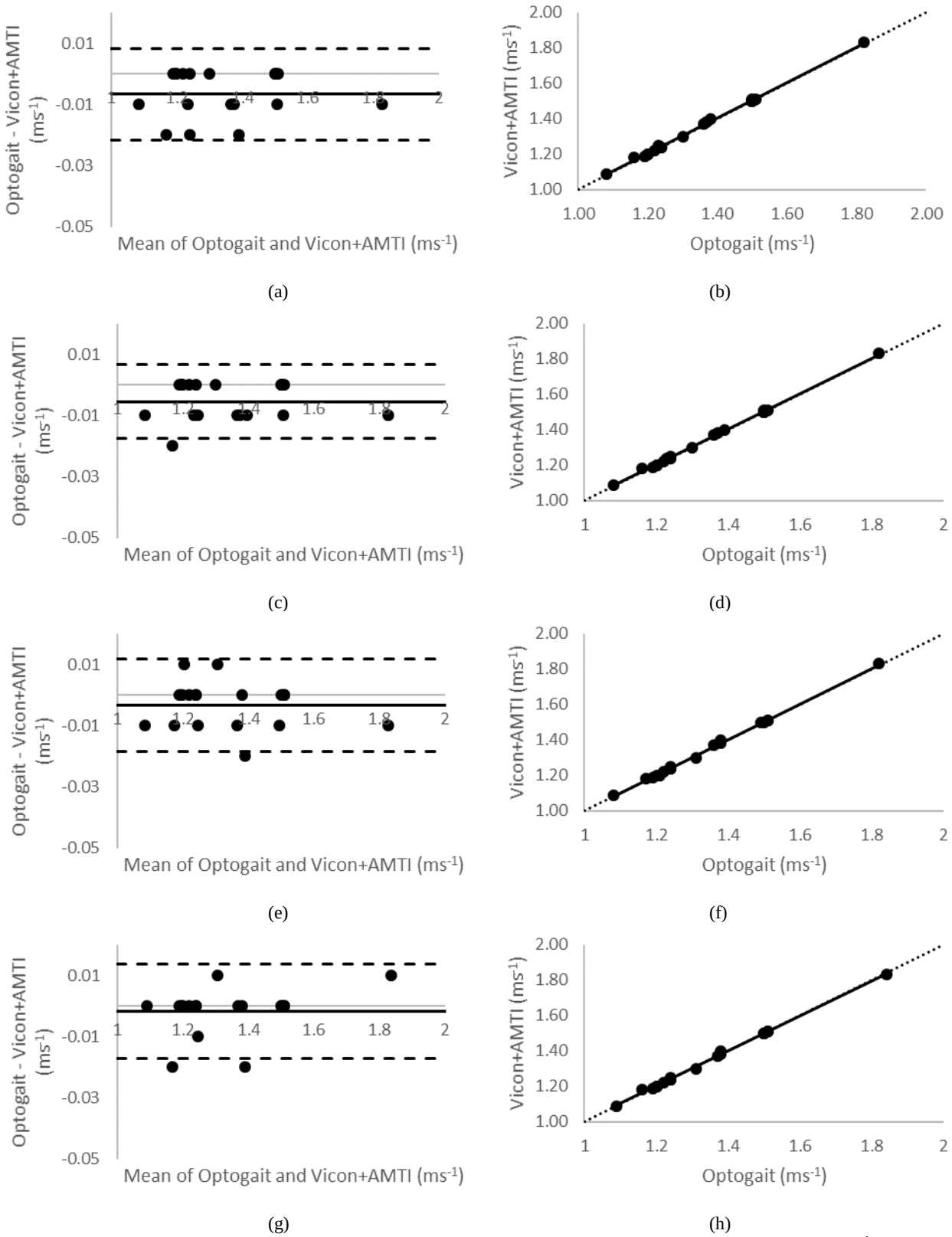

Supplementary Figure 15: Bland–Altman plots and scatterplots for left walking speed (ms^{-1}) Vicon+AMTI against 0 LED (a and b), 1 LED (c and d), 2 LED (e and f) and 3 LED (g and h). On the Bland–Altman plots, the solid line represents the bias and the broken lines represent the upper and lower 95% Limits of Agreement. On the scatterplots, the solid line represents the linear regression line and the dotted line represents the identity line.

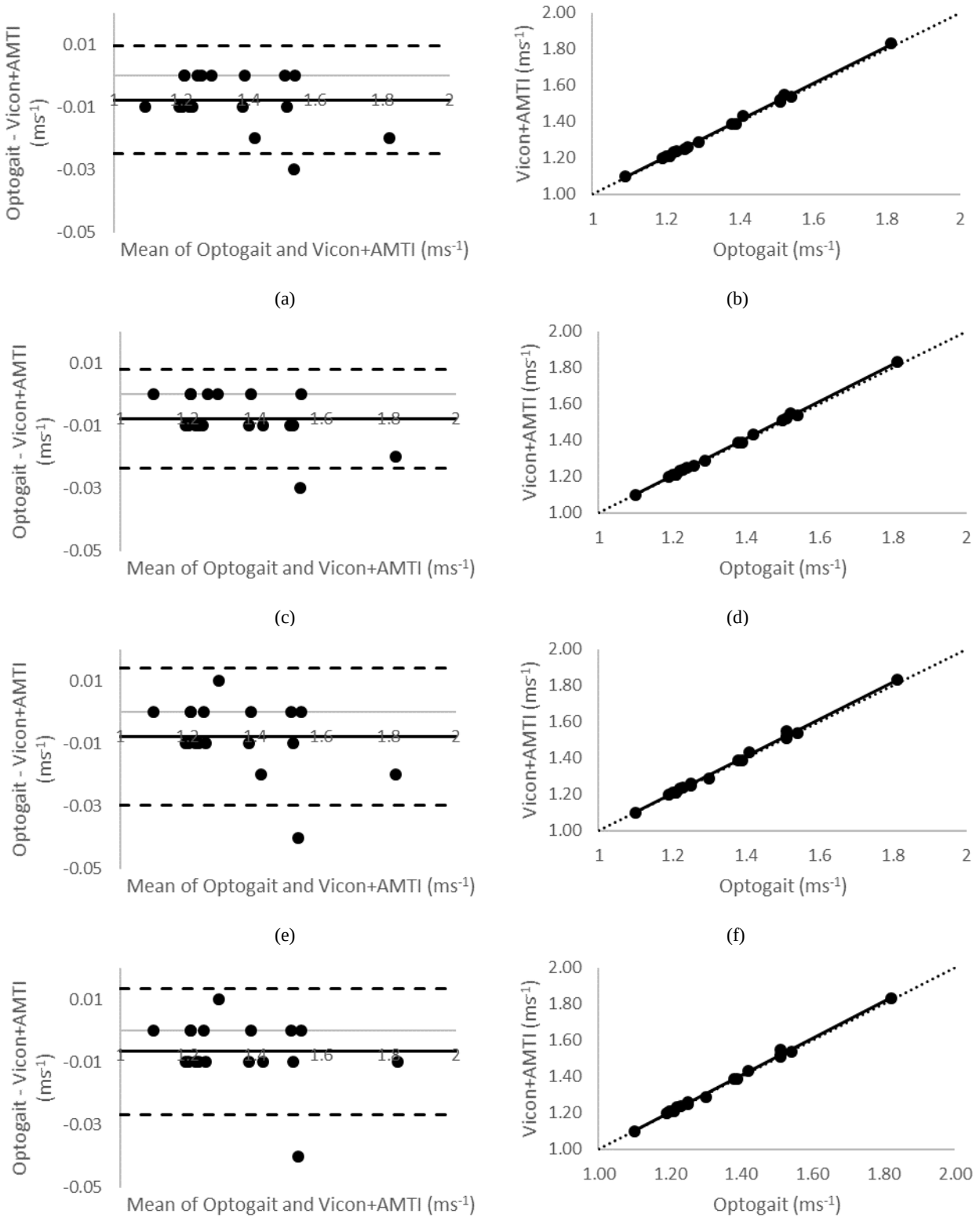

Supplementary Figure 16: Bland–Altman plots and scatterplots for right walking speed (ms^{-1}) Vicon+AMTI against 0 LED (a and b), 1 LED (c and d), 2 LED (e and f) and 3 LED (g and h). On the Bland–Altman plots, the solid line represents the bias and the broken lines represent the upper and lower 95% Limits of Agreement. On the scatterplots, the solid line represents the linear regression line and the dotted line represents the identity line.

Supplementary Table 1: Statistical analysis results for repeated measures ANOVA with a Greenhouse-Geisser correction.

Gait parameter		df1	df2	F-statistic	p-value
Stance phase	Left	1.466	24.921	49.503	< 0.001
	Right	2.069	35.176	48.828	< 0.001
Swing phase	Left	1.498	25.466	40.234	< 0.001
	Right	2.413	41.025	30.052	< 0.001
Walking speed	Left	3.103	52.745	6.086	0.001
	Right	1.845	31.362	7.750	0.002

Supplementary Table 2: Statistical analysis results for post hoc tests using the Bonferroni correction.

Gait parameter		Vicon+AMTI versus OptoGait (0 LED) p-value	Vicon+AMTI versus OptoGait (1 LED) p-value
Stance phase	Left	< 0.001	< 0.001
	Right	< 0.001	< 0.001
Swing phase	Left	< 0.001	0.003
	Right	< 0.001	0.011
Walking speed	Left	0.018	0.013
	Right	0.016	0.008